Introducing low-cost pyrazine unit into terpolymer enables high-performance polymer solar cells with efficiency of 18.23%

Liuyang Zhou[a,b], *Lei Meng*[a,b*], *Jinyuan Zhang*[a*], *Can Zhu*[a,b], *Shucheng Qin*[a,b], *Indunil Angunawela*[d], *Yan Wan*[e], *Harald Ade*[d*], *Yongfang Li*[a,b,c*]

[a] *Beijing National Laboratory for Molecular Sciences, CAS Key Laboratory of Organic Solids, Institute of Chemistry, Chinese Academy of Sciences, Beijing, 100190, China*

[b] *School of Chemical Science, University of Chinese Academy of Sciences, Beijing, 100049,China*

[c] *Laboratory of Advanced Optoelectronic Materials, College of Chemistry, Chemical Engineering and Materials Science, Soochow University, Suzhou, Jiangsu, 215123, China*

[d] *Department of Physics and Organic and Carbon Electronics Lab, North Carolina State University, Raleigh, North Carolina 27695, United States*

[e] *College of Chemistry, Beijing Normal University, Beijing 100875, China*

***Corresponding authors:**

menglei@iccas.ac.cn (L.Meng), zhangjinyuan@iccas.ac.cn (J. Zhang), hwade@ncsu.edu (H. Ade), liyf@iccas.ac.cn (Y. Li)

Abstract

Random ternary copolymerization strategy becomes a promising and efficient approach to develop high-performance polymer donors for polymer solar cells (PSCs) recently. In this work, we incorporated a low-cost electron-withdrawing unit, 2,5-bis(4-(2-ethylhexyl)thiophen-2-yl)pyrazine (PZ-T), into polymer backbone of PM6 as the third component, and synthesized three D-A_1-D-A_2 type terpolymers PMZ-10, PMZ-20 and PMZ-30 by the random copolymerization strategy, with the PZ-T proportion of 10%, 20% and 30%, respectively. The terpolymers exhibit downshifted highest occupied molecular orbital (HOMO) energy levels than PM6, which is beneficial for obtaining higher open-circuit voltage (V_{oc}) of the PSCs with the polymer as donor. Importantly, the PSCs based on PMZ-10:Y6 demonstrate efficient exciton dissociation, higher and balanced electron/hole mobilities, desirable aggregation, and high power conversion efficiency (PCE) of 18.23%, which is the highest efficiency among the terpolymer-based PSCs so far. The results indicate that the ternary copolymerization strategy with PZ-T as the second A-unit is an efficient approach to further improve the photovoltaic performance and reduce the synthetic cost of the D-A copolymer donors.

Keywords

Polymer solar cells; conjugated polymer donors; pyrazine unit; terpolymers; ternary random copolymerization.

Introduction

Polymer solar cells (PSCs), composed of a *p*-type conjugated polymer donor and a *n*-type organic semiconductor polymer or small molecule acceptor, have developed rapidly and drawn considerable attentions due to their merits including solution-processability, simple device structure, light-weight and flexibility[1-9]. The complementary absorption in the visible to near infrared region, the electronic energy levels matching and the appropriate morphology of the donor and acceptor materials in the blend active layer, are very important for realizing high power conversion efficiency (PCE) of the PSCs. In recent years, PCE of the PSCs has increased quickly, which is mainly benefitted from the development of the narrow bandgap small molecule acceptors (SMAs)[10-17] and the wide bandgap conjugated polymer donors[18-25]. Especially, the emergence of the A-DA'D-A structured SMA Y6 developed by Zou *et al.*[8, 12], greatly improved the PCE of the PSCs to over 17~18%[26-28] recently.

Currently, the most representative high-performance polymer donor for the Y6-based PSCs is the wide bandgap D-A copolymer PM6[29], with the bi(alkyl-fluoro-thienyl)-benzodithiophene (BDTT) as D-unit and 1,3-bis(thiophen-2-yl)-5,7-bis(2-ethylhexyl)benzo[1,2-c:4,5-c0]dithiophene-4,8-dione (BDD) as A-unit. While the PCE of the PSCs based on PM6:Y6 is only *ca*. 16%, and the synthetic cost of PM6 is high due to the complicated multi-synthetic steps of the BDTT D-unit and the BDD A-unit. Therefore, further improving the photovoltaic performance and reducing the synthetic cost of PM6 is of great significance in facilitating the commercialization of the PSCs.

In order to improve the photovoltaic performance of PM6, ternary random D-A copolymerization strategy has been proposed by introducing a third component into the original binary D-A backbone of PM6, including the D_1-A-D_2-A type terpolymers with another electron-donating unit (D_2) as the third component[30-33] and the D-A_1-D-A_2 type terpolymers with another electron-accepting unit (A_2) as the third component[34-40]. By controlling the proportion of the third component, the energy levels and absorption properties of the target terpolymers can be effectively tuned without compromising the desired blend morphology of the active layer. For instance, in 2019, Hou[37] *et al.* incorporated the ester-substituted thiophene (EST) as A_2-unit into PM6, and the resulted terpolymer showed downshifted electronic energy levels and broadened absorption. The PSC based on terpolymer T1 (with 20% proportion of EST) as donor and IT-4F as acceptor demonstrated over 15% PCE. In 2020, Zhang[38] *et al.* incorporated thiophene-thiazolothiazole (TTZ) as A_2-unit with 20% proportion into the PM6 polymer backbone and obtained a D-A_1-D-A_2-type random terpolymers (named as PM1), which shows lower HOMO energy level, higher hole mobility and more favorable morphology. The PSC based on PM1:Y6 achieved high PCE of 17.6%. In the same year, Zhang[39] *et al.* also incorporated 20% of the 5, 5'-dithienyl-2,2'-bithiazole (DTBTz) as A_2-unit into the backbone of PM6, and obtained a new terpolymer named as PM6-Tz20, which could effectively tailor the molecular orientation and aggregation, and optimize the active layer morphology. Then, the devices based on PM6-Tz20:Y6 achieved PCE of 17.6%.

In this work, we designed and synthesized a weakly electron-withdrawing unit, 2,5-bis(4-(2-ethylhexyl)thiophen-2-yl)pyrazine (PZ-T), and incorporated PZ-T as A2-unit into the polymer backbone of PM6 to obtain three D-A_1-D-A_2 type terpolymers by random copolymerization strategy. PZ-T was synthesized by two simple steps with high yield from low cost raw materials. The three terpolymers are PMZ-10, PMZ-20 and PMZ-30 (**Figure**

1a) with PZ-T proportion of 10%, 20% and 30%, respectively. Compared with PM6, the three terpolymers exhibit gradually down-shifted HOMO energy levels and higher absorption coefficient, which could lead to higher V_{oc} and short-circuit current density (J_{sc}) for the corresponding PSCs. When blended with Y6 acceptor, the terpolymers-based active layers demonstrated proper aggregation, desirable crystallinity and balanced electron/hole mobilities, which would be beneficial for higher FF of their PSCs. Eventually, the device based on PMZ-10:Y6 achieved the highest PCE of 18.23%, with a V_{oc} of 0.834 V, a large J_{sc} of 27.96 $mAcm^{-2}$, and a higher FF of 78.2%, which is the highest PCE among the terpolymer-based PSCs so far. And the devices based on PMZ-20:Y6 and PMZ-30:Y6 also obtained higher PCE of 17.64% and 17.17%, respectively, compared to the device based on PM6:Y6 (PCE of 16.63%). The results demonstrate that the ternary copolymerization strategy is a promising and efficient approach to further enhance the photovoltaic performance of the PM6-based PSCs.

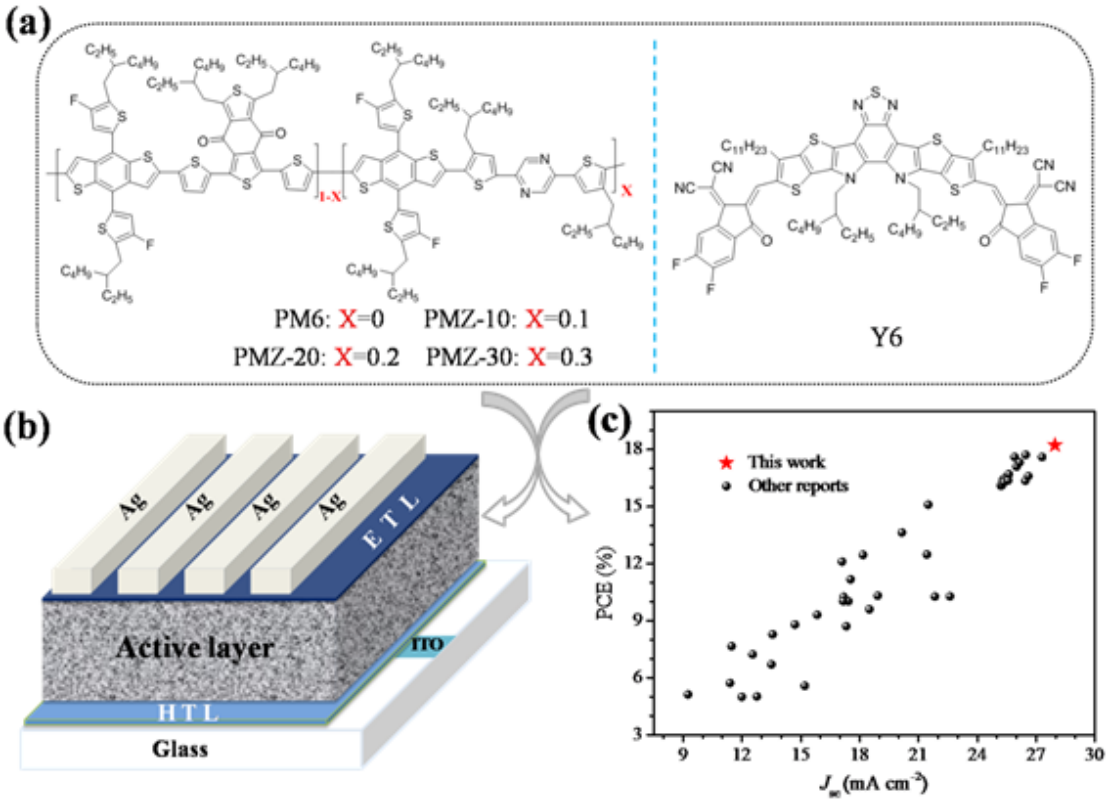

Figure 1. a) Chemical structures of the polymer donors and Y6 acceptor. b) Device structure of the PSCs. c) Scatter plot of the PCE and J_{sc} values for the efficient terpolymer based PSCs reported in literatures and in this work (labeled as a red star).

Results and Discussion

The random terpolymers were synthesized by Stille coupling polymerization with three monomers including the electron-rich 4,8-bis(5-(2-ethylhexyl)-4-fluorothiophen-2-yl)benzo[1,2-*b*:4,5-*b*′]-dithiophene (BDT-F) D-unit and electron-deficient 1,3-bis(thiophen-2-yl)-5,7-bis(2-ethylhexyl)benzo-[1,2-*c*:4,5-*c*′]dithiophene-4,8-dione (BDD) A_1-unit and 2,5-bis(5-bromo-4-(2-ethylhexyl)thiophen-2-yl)-pyrazine (PZ-T-Br) A_2-unit. Four polymer donors PM6, PMZ-10, PMZ-20 and PMZ-30 were synthesized with the PZ-T proportion of

0%, 10%, 20% and 30%, respectively. The synthetic routes for monomer PZ-T-Br and the four polymer donors were shown in **Scheme S1** in supporting information (SI). The monomer PZ-T-Br was obtained with high yield by two simple steps of Stille coupling and bromination reactions. Moreover, the starting material of 2,5-dibromopyrazine (PZ-Br) is low-cost, and would reduce the overall synthetic cost of the terpolymers. Optimized batches of the polymer donors were obtained by controlling the polymerization conditions, and all of the polymers exhibited good solubility in common organic solvents, such as chloroform (CF), chlorobenzene (CB), and dichlorobenzene (DCB) *etc*. The number-average molecular weights (M_n) of the polymer donors were measured by high-temperature gel permeation chromatography (HT-GPC) with 1,3,5-trichlorobenzene as the eluent. The M_n of PM6, PMZ-10, PMZ-20, PMZ-30 were measured to be 36.80 kDa, 35.94 kDa, 29.44 kDa and 28.26 kDa, with corresponding polydispersity index (PDI) of 2.13, 2.21, 2.29 and 2.30, respectively (**Table 1**, **Figure S1a-d**).

Thermal stability of the polymer donors was characterized by thermogravimetric analysis (TGA). As shown in **Figure S2d**, PM6 and PMZ-10 exhibit similar thermal stability with 5% weight loss at temperature of 418°C and 417°C, respectively. With the increase of PZ-T proportion, the terpolymers of PMZ-20 and PMZ-30 show slightly lower decomposition temperature (with weight loss of 5%) at 402°C and 376°C. Even though, the thermal stability of PMZ-20 and PMZ-30 is still sufficient for the application as donor in the PSCs.

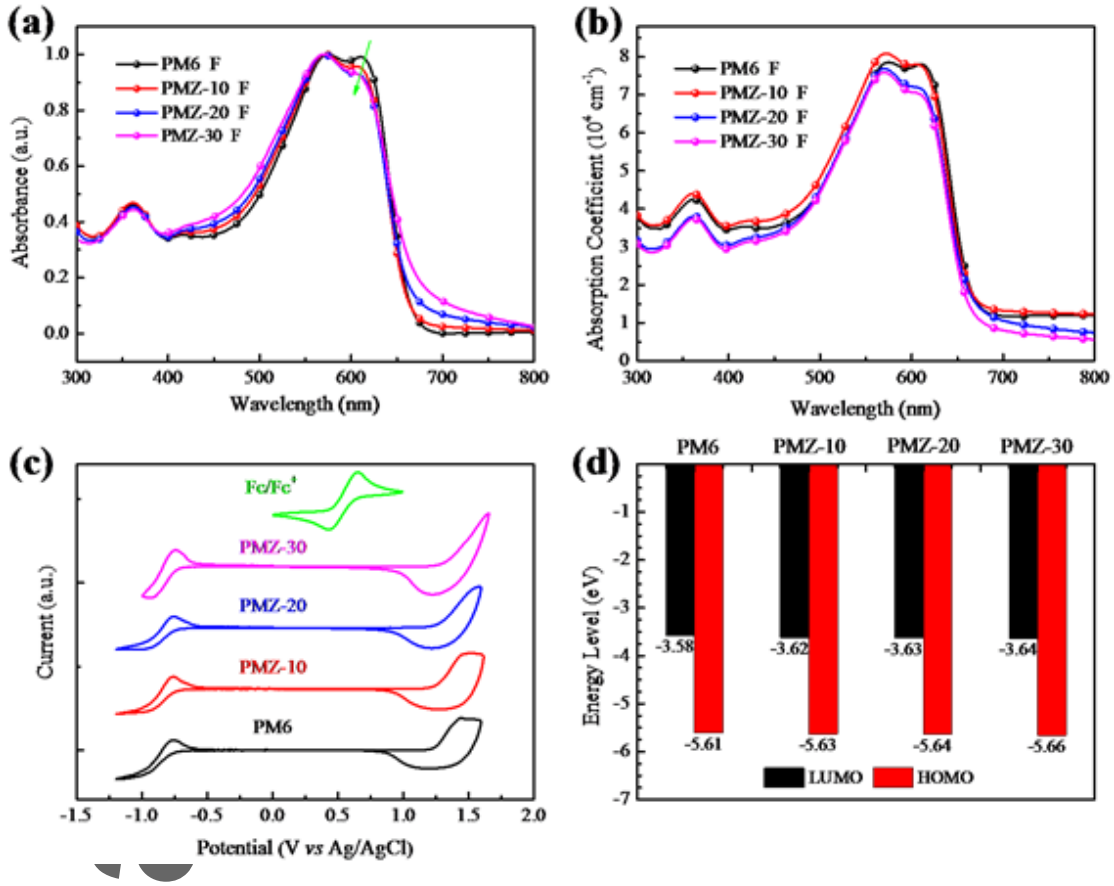

Figure 2. a) Normalized absorption spectra and b) corresponding absorption coefficients of the neat polymer donor films. c) Cyclic Voltammograms of the polymer donors. d) Schematic energy level diagram of the polymer donors.

Figure 2a and **Figure S2a** in SI show the UV-Vis absorption spectra of the four polymer donors in thin films and CF solutions respectively, and the corresponding data of the optical properties were summarized in **Table 1**. In both film and solution states, these polymers demonstrate gradually blue-shifted absorption with increasing proportion of PZ-T in the terpolymers. All neat polymer films show similar absorption onsets at about 675 nm with the optical bandgap of 1.84 eV, and similar π-π* transition (300~400 nm) peaks and intramolecular charge transfer (ICT) (500~700 nm) peaks. Meanwhile, PM6 exhibits

pronounced shoulder peaks at about 573 nm and 612 nm, corresponding to the 0-1 and 0-0 transitions. With the increase of PZ-T proportion, the 0-0 transition peak is gradually weakened for neat and blend films (**Figure S2b**), which is ascribed to the weaker ICT and aggregation behavior[41, 42]. Moreover, the neat film of PMZ-10 shows slightly higher absorption coefficient (8.11×10^4 cm^{-1}) than PM6 (7.87×10^4 cm^{-1}) (**Figure 1b**). Similarly, the blend films (**Figure S2c**) of PMZ-10:Y6 also demonstrate enhanced absorption coefficient, which could lead to better light-harvesting.

The cyclic voltammetry (CV) measurement was carried out to estimate the energy levels of the polymer donors PM6, PMZ-10, PMZ-20 and PMZ-30 (**Figure 2c**). The HOMO and LUMO energy levels were calculated by the equations of $E_{HOMO/LUMO} = -e\,(E_{ox/red} + 4.8 - E_{Fc/Fc^+})$ (eV), where the $E_{ox/red}$ represents the onset oxidation and onset reduction potentials with unit of V *vs*. Ag/AgCl, respectively, and the redox potential of ferrocene E_{Fc/Fc^+} is used as an internal standard and was measured to be 0.44 eV *vs*. Ag/AgCl. Finally, the equations were simplified as $E_{HOMO/LUMO} = -e\,(E_{ox/red} + 4.36)$ (eV). As shown in **Figure 2d**, with the increase of PZ-T proportion, the HOMO/LUMO energy levels of the terpolymers gradually downshifted compared with PM6, as shown in **Table 1**. The E_{HOMO}/E_{LUMO} values of PM6, PMZ-10, PMZ-20 and PMZ-30 are determined as −5.61/−3.58 eV, −5.63/−3.62 eV, −5.64/−3.63 eV and −5.66/−3.64 eV, respectively, which matches well with that of Y6 acceptor (−5.70/−4.10 eV).

Table 1. Molecular weights, optical properties and electronic energy levels of the polymer donors.

Polymer Donor	M_n (kDa)	PDI	λ_{max}^{film} (nm)	λ_{onset}^{film} (nm)	$E_g^{opt.}$(eV)[a]	E_{HOMO}(eV)[b]	E_{LUMO}(eV)[b]

PM6	36.80	2.13	575	678	1.83	-5.61	-3.58
PMZ-10	35.94	2.21	574	674	1.84	-5.63	-3.62
PMZ-20	29.44	2.29	573	672	1.85	-5.64	-3.63
PMZ-30	28.26	2.30	572	671	1.85	-5.66	-3.64

[a] Optical band-gap was calculated from E_g^{opt}=1240/λ_{onset}.

[b] Estimated from the onset oxidation/reduction potentials on the CV curves.

The effect of the PZ-T proportion on the photovoltaic properties of the terpolymers donors were investigated by fabricating PSCs with conventional device structure of ITO (indium tin oxide)/PEDOT:PSS (poly(3,4-ethylenedioxythiophene):poly(styrene-sulfonate))/Polymer donor:Y6/PNDIT-F_3N/Ag (see **Figure 1b**). Firstly, the devices based on the terpolymers with different proportions of PZ-T were optimized by tuning the D/A ratio (*w/w*), dosage of additive and temperatures of thermal annealing (TA) treatment, and the results were summarized in **Table S1**. **Figure 3a** shows the current density−voltage (*J-V*) curves of the optimized devices, and **Table 2** lists the detailed photovoltaic parameters of the corresponding PSCs for a clear comparison. As expected, the V_{oc} was enhanced with the increase of PZ-T proportion in the terpolymer donor, which is consistent with the downshift of E_{HOMO} of the polymer donors. Eventually, the optimized devices based on PMZ-10:Y6 exhibit an excellent PCE of 18.23%, with V_{oc} of 0.834 V, J_{sc} of 27.96 mA cm^{-2} and FF of 78.2%, where the PCE is the highest reported value among the terpolymers-based PSCs and the J_{sc} is also one of the highest in the PSCs so far (**Figure 1c**). Meanwhile, the photovoltaic performance of PMZ-10 possesses better reproducibility with different molecular weight, as listed in **Table S2**, which is very important to explore high-performance polymer donors for

the application of PSCs. In addition, a certified PCE of 17.75% was obtained from National Institute of Metrology (NIM) (certificate is included in **Figure S3**). The control devices based on PM6:Y6 show relatively lower PCE of 16.63%, with V_{oc} of 0.825 V, J_{sc} of 26.80 mA cm^{-2} and FF of 75.2%. With further increasing proportion of PZ-T to 20% in PMZ-20 and 30% in PMZ-30, the devices based on PMZ-20:Y6 and PMZ-30:Y6 also obtained decent photovoltaic performance with PCE of 17.64% (V_{oc} of 0.841 V, J_{sc} of 27.39 mA cm^{-2}, FF of 76.6%) and 17.17% (V_{oc} of 0.847 V, J_{sc} of 26.92 mA cm^{-2}, FF of 75.3%), respectively. The slightly lower PCEs of the PSCs based on the terpolymers of PMZ-20 and PMZ-30 could be ascribed to the slightly reduced J_{sc} and FF. The above results indicate that the terpolymer strategy is an effective approach for achieving high-performance PSCs. It should be mentioned that we also synthesized PMZ-100 with 100% PZ-T A-unit in the polymer for investigating the effect of 100% content of the PZ-T A-unit on its photovoltaic performance. However, the PCE of the PSC based on PMZ-100:Y6 is only 8.27% with a higher V_{oc} of 0.871 V, but lower J_{sc} of 18.51 and lower FF of 54.49% (as shown in Table S1), due probably to its too low HOMO energy level, weaker 0-0 transition peak of PMZ-100 and poorer complementary absorption of PMZ-100:Y6 active layer (Figure S4 (a)) and too strong aggregation as shown in the large RMS roughness value of 4.52 nm in its AFM hight image (Figure S4 (b))

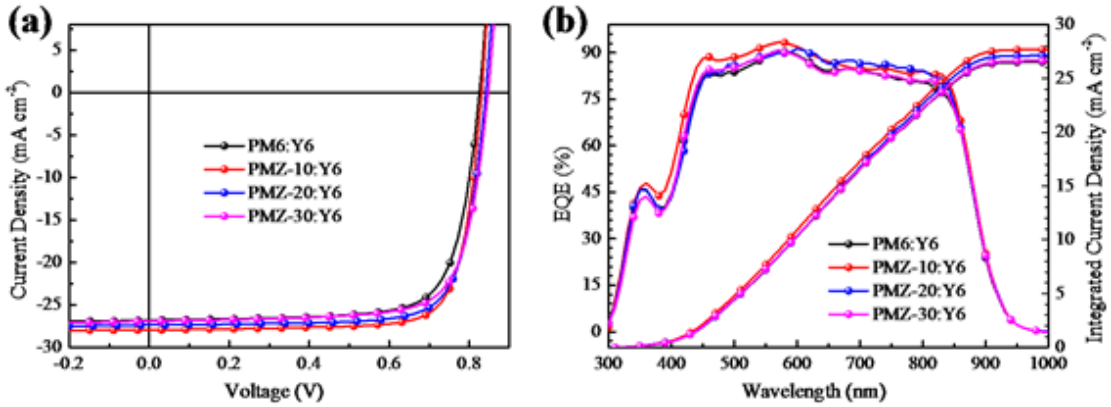

Figure 3. a) *J*−*V* curves of the optimized PSCs under illumination of AM1.5G, 100 mW cm^{-2}. b) EQE curves and corresponding integrated current densities of the PSCs.

Figure 3b shows the external quantum efficiency (EQE) spectra of the optimized devices, and all the devices display a broad and high photoresponse in the wavelength range of 300~950 nm. Especially, the device based on PMZ-10:Y6 exhibits higher responses from 450 nm to 650 nm with EQE response exceeding 85% and the peak value reached 93% at 575 nm, which surpasses the other three devices based on PM6:Y6, PMZ-20:Y6 and PMZ-30:Y6. The integrated J_{sc} values of the devices based on PM6:Y6, PMZ-10:Y6, PMZ-20:Y6 and PMZ-30:Y6 were 26.53 mA cm^{-2}, 27.68 mA cm^{-2}, 27.12 mA cm^{-2} and 26.65 mA cm^{-2}, respectively, which agrees well with those obtained from the *J*−*V* curves within 1% mismatch.

Table 2. The photovoltaic performances parameters of the optimized PSCs based on polymer donors:Y6 blend films with thermal annealing treatment at 110°C for 10 min, under the illumination of AM1.5G, 100 mW cm^{-2}.

Donor:acceptor[a]	V_{oc}(V)[b]	J_{sc}(mA cm^{-2})[b]	FF(%)[b]	PCE(%)[b]

PM6:Y6	0.825 (0.823±0.002)	26.80 (26.63±0.19)	75.2 (74.6±0.7)	16.63 (16.49±0.16)
PMZ-10:Y6	0.834 (0.832±0.002)	27.96 (27.74±0.23)	78.2 (77.8±.0.5)	18.23 (18.15±0.11)
PMZ-20:Y6	0.841 (0.838±0.003)	27.39 (27.21±0.18)	76.6 (75.9±1.0)	17.64 (17.51±0.13)
PMZ-30:Y6	0.847 (0.844±0.003)	26.92 (26.61±0.29)	75.3 (74.8±0.6)	17.17 (17.04±0.15)

[a] All devices were fabricated with D/A weight ratio of 1:1.2 and with additive treatment of 0.5% chloronaphthalene (CN).

[b] The average values with standard deviation in parentheses were obtained from more than 15 devices.

To provide insights of the influence of PZ-T proportions on the charge recombination dynamics of the terpolymer donors, the relationship of J_{sc} and V_{oc} as a function of the light intensity (P_{light}) were measured and analyzed. Firstly, the function of log J_{sc} *vs* log P_{light} was plotted to investigate the bimolecular recombination behavior in the PSCs (**Figure 4a**). The relationship between J_{sc} and P_{light} follows the equation of $J_{sc} \propto P_{light}^{\alpha}$[43], where α is the exponential factor. When α value is close to unity, bimolecular recombination is suppressed at the short-circuit condition in the devices. The α value of the device based on PMZ-10:Y6 is measured to be 0.994, which is closer to unity than other devices based on PM6:Y6, PMZ-20:Y6 and PMZ-30:Y6, with corresponding α values of 0.973, 0.986 and 0.978, respectively. The higher α value indicates suppressed bimolecular recombination to a large extent and leads to higher FF, which also agrees well with the device performance of the PSCs. In addition, the relationship between V_{oc} and P_{light} can be described by the formula of $V_{oc} \propto nkT/q\ln P_{light}$ (**Figure 4b**), where k, T and q represent Boltzmann constant, Kelvin

temperature and elementary charge, respectively. When the bimolecular recombination dominates, the values of n should be close to 1; when n is close to 2, the monomolecular or trap-assisted recombination in the film dominates[44]. In this study, the curves of V_{oc} *vs.* lnP_{light} for the devices based on PMZ-10:Y6, PMZ-20:Y6 and PMZ-30:Y6 display relatively lower slopes of 1.11kT/q, 1.15kT/q and 1.20kT/q, respectively. As a comparison, for devices based on PM6:Y6, a slightly higher slope of 1.26kT/q was obtained. The results also indicate the effective suppression of monomolecular recombination when introducing PZ-T units into PM6.

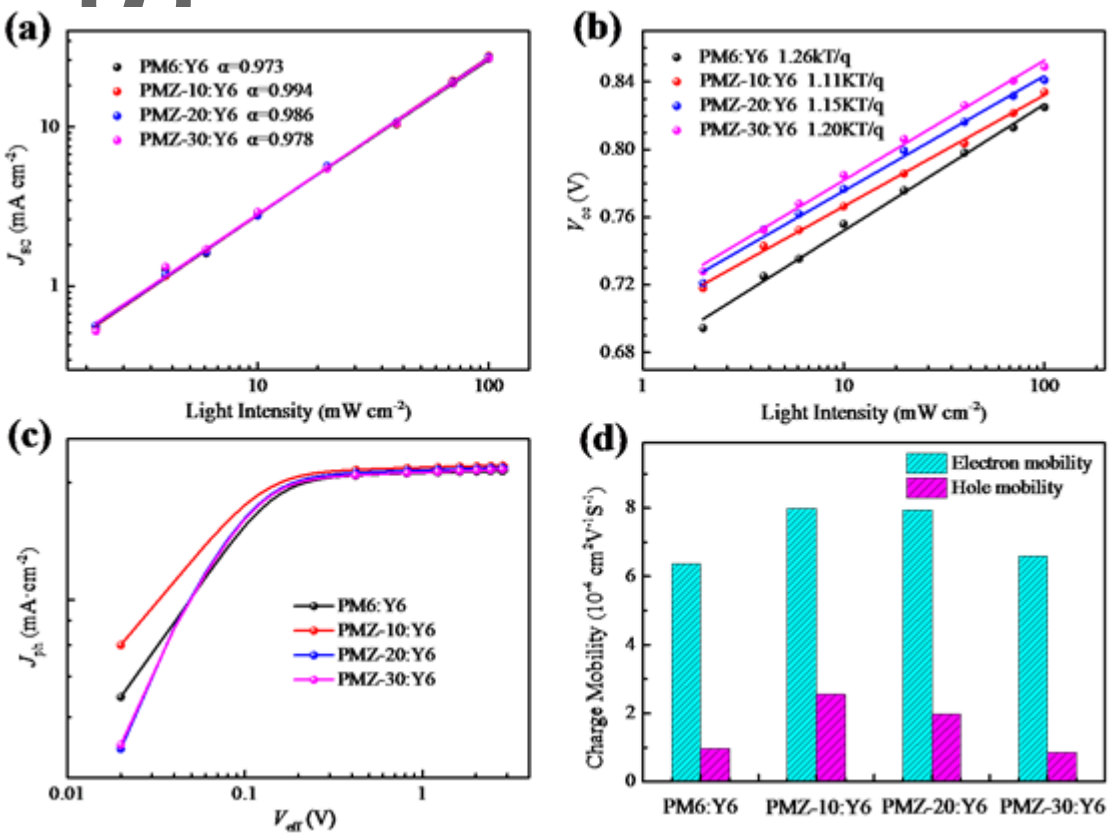

Figure 4. a) J_{sc} and b) V_{oc} dependence on the light intensity of the corresponding PSCs. c) $J_{ph}-V_{eff}$ characteristics of the PSCs. d) The charge carrier mobility of the blend films based on polymer donors:Y6.

To better understand the effect of PZ-T proportions in the terpolymers on the exciton dissociation process in the active layer, the dependence of photocurrent density (J_{ph}) on the effective voltage (V_{eff}) was measured for the optimized devices, as shown in **Figure 4c**. In the measurements, $J_{ph} = J_L - J_D$, where J_L and J_D are the current density under light irradiation and in the dark, respectively. $V_{eff} = V_0 - V_{bias}$, where V_0 and V_{bias} are the voltage at $J_L = J_D$ and the applied bias voltage, respectively. The exciton dissociation efficiency (P_{diss}) could be calculated according to the formula of $P_{diss} = J_{ph}/J_{sat}$ under short-circuit condition. When $V_{eff} \geq 2$ V[45], the charge carriers were quickly collected to the electrodes and J_{ph} reaches saturation (J_{sat}). Consequently, the P_{diss} values were estimated to be 98.37%, 98.88%, 98.52% and 98.29%, for the devices based on PM6:Y6, PMZ-10:Y6, PMZ-20:Y6 and PMZ-30:Y6, respectively. These results indicate that all the four devices show efficient exciton dissociation, while the PMZ-10-based device possesses the most efficient exciton dissociation, which could explain the highest J_{sc} and FF of the PMZ-10-based device.

To investigate the charge transport properties of the neat polymer and polymers:Y6 blend films, the electron mobility (μ_e) and hole mobility (μ_h) were measured by space-charge-limited-current (SCLC) method, with the device structures of ITO/ZnO/blends/PNDIT-F_3N/Ag and ITO/PEDOT:PSS/polymers or blends/MoO_3/Ag, respectively. The $J^{1/2} - V$ curves were shown in **Figure S5a-c**, and corresponding charge carrier mobilities calculated from the curves are shown in **Figure 4d**, **Figure S5d** and **Table S3**, respectively. Among the four neat polymer films, the PMZ-10 film exhibits the highest μ_h of 3.21×10^{-4} cm^2 V^{-1} s^{-1}. Meanwhile, the PMZ-10:Y6 blend film also possesses the highest μ_h of 2.55×10^{-4} and μ_e of 7.99×10^{-4} cm^2 V^{-1} s^{-1}. Compared with PM6:Y6 blend film, PMZ-10:Y6 film achieves simultaneously improved μ_h and μ_e, and more balanced charge carrier transport with a lower μ_e/μ_h ratio of 3.13, which might result in the higher J_{sc} and FF in the PSCs based on PMZ-10:Y6.

In addition, transient photocurrent (TPC) measurements were carried out to study space-charge effects and carrier trapping in the PSCs. As shown in **Figure S6**, the devices based on PMZ-10:Y6 exhibit faster rise and fall response to the light pulse, which indicates that the charge extraction is more rapid and trap density in the blend film is relatively low. The less carrier trapping is beneficial to increase the charge generation and reduce the non-radiative recombination, leading to the higher V_{oc} and J_{sc} in the PSCs.

To understand the effect of PZ-T units on the morphology of the terpolymer-based blend films, atomic force microscopy (AFM) and transmission electron microscopy (TEM) were employed to investigate the surface and bulk morphology of the blend films. AFM height images with the size of 1×1 μm^2 and 5×5 μm^2 were shown in **Figure 5a-d** and **Figure S7a-d**, respectively. As can be seen from the 1×1 μm^2 size images, PMZ-10:Y6 blend film exhibits finer nanoscale fibrillar texture with a slightly larger root-mean-square (RMS) roughness value of 0.91 nm compared with PM6:Y6, which contributes to efficient exciton dissociation and charge transport. With the increase of PZ-T proportion, the RMS roughness increased gradually to 0.95 nm and 1.06 nm corresponding to PMZ-20:Y6 and PMZ-30:Y6 blend films, respectively. After incorporating PZ-T with 20% proportion, obvious aggregation tendency of the blend film based on PMZ-20:Y6 was observed compared to the PM6:Y6-based blend film. Furthermore, by introducing PZ-T proportion to 30%, the PMZ-30:Y6 film exhibits weaker phase separation, which results in lower exciton dissociation efficiency and leads to gradually decreased FF. Similar results could also be observed in the TEM images (**Figure S7e-h**), the bright and dark domains were observed from the terpolymer-based active layers, indicating the increased phase separation in the blend films based on the PZ-T incorporated terpolymers.

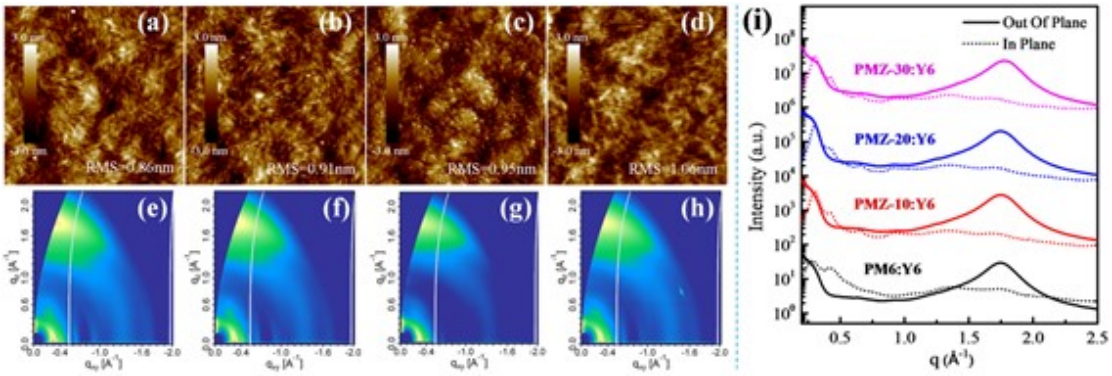

Figure 5. AFM height images (1×1 μm^2) (a-d) and 2D-GIWAXS images (e-h) of the blend films based on: a), e) PM6:Y6;b), f) PMZ-10:Y6;c), g) PMZ-20:Y6; d), h) PMZ-30:Y6; i) Corresponding 1D line-cuts in the In-plane (IP) and Out-of-plane (OOP) direction.

To further understand the effect of the third component PZ-T of the terpolymer on the film molecular packing, an in-depth study was conducted by grazing incident wide-angle X-ray scattering (GIWAXS)[46]. The 2D GIWAXS patterns and corresponding 1D intensity profiles were shown in **Figure 5e-i** and **Figure S8a-f**, and the fitting results are summarized in **Table S4-S5**. All the original polymer films were prepared under identical conditions. The neat polymer films exhibit pronounced π-π stacking (010) peaks in the out-of-plane (OOP) direction, which indicates that the neat films displayed more preferential face-on orientation in the vertical direction of substrate, and they exhibit similar π-π stacking distance (d) (q_z=1.69 Å^{-1}, d=3.73 Å) and π-π stacking coherence length (CCL) ($\triangle q_z$≈0.31 Å^{-1}, CCL≈20 Å), which means that the terpolymers still maintain the quality of the molecular ordering of PM6. In the blend films, the OOP π-π stacking is more prominent than that of in-plane (IP) with distinct (010) diffractions, which implies that the blend films are predominantly face-on orientation, which contributes to efficient charge transport in the vertical direction. The π-π stacking distance in the PMZ-10:Y6 blend film showed no distinct difference from PM6:Y6 film but slightly higher normalized integrated intensity of the π-π stacking compared with

PM6:Y6. Furthermore, the PMZ-30:Y6 blend has the obviously larger donor π-π stacking distance, indicating that the ordering of the aggregates was disturbed with the increased proportion of PZ-T units after a certain limit. Therefore, introducing PZ-T units could affect the molecular packing and ordering behavior of PM6 to some extent, and the more proper crystallinity could contribute to the enhanced charge transport and higher FF in the PSCs.

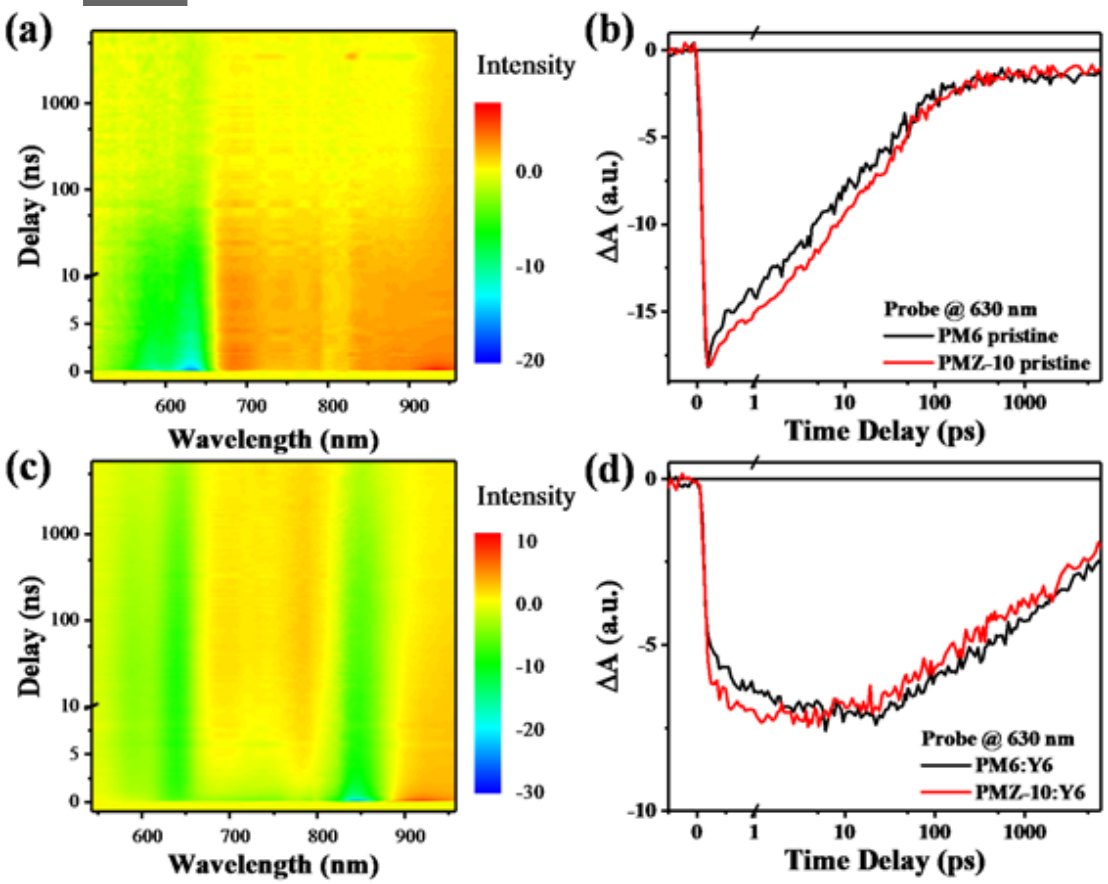

Figure 6. Femtosecond transient absorption spectra of a) PMZ-10 pristine film with excitation at 600 nm. b) kinetic trace of PM6 and PMZ-10 pristine films probing at 630 nm. c) PMZ-10:Y6 blend film with excitation at 850 nm. d) kinetic trace of PM6:Y6 and PMZ-10:Y6 blend films probing at 630 nm.

To get a better insight into the charge transfer (CT) and recombination dynamics of the active layer, femtosecond transient absorption spectroscopy (fs-TA) was carried out on PM6 and PMZ-10 pristine films and the PM6:Y6 and PMZ-10:Y6 blend films (shown in **Figure S9**).At first, we studied the excited state dynamics of the polymer donors PMZ-10 and PM6 by photoexciting the pristine film with pump wavelength at 600 nm. **Figure 6a** shows the fs-TA spectra of PMZ-10. The absorption of PMZ-10 exciton consists of a negative ground state bleach (GSB) with peak at 630 nm, and a very broad excited state absorption (ESA) ranging from 670 nm to 950 nm. As shown in **Figure 6b**, the decay kinetics of PMZ-10 excitons exhibits a longer lifetime (55 ps) than that of PM6 exciton (42 ps), the relatively longer exciton lifetime of PMZ-10not only improves the exciton diffusion length, but also promotes exciton dissociation efficiency in the blend film[47, 48].

Then we investigated the CT behavior of the active layers by selectively exciting the Y6 acceptor at 850 nm in both blend films. As shown in **Figure 6c**, upon excitation, a broad GSB signal with a peak at 810 nm was observed, resulting from the Y6 exciton. Another GSB signal also appeared at 630 nm simultaneously, which matches the absorption of the polymer donor PMZ-10, ascribed to the CT state resulting from the ultrafast hole transfer from Y6 exciton to PMZ-10. The intensity of GSB signal of PMZ-10 at 630 nm continued to increase rapidly to a maximum after the initial sharp rise, then it started to decay slowly, suggesting that the CT state builds up its population by exciton diffusion after the ultrafast hole transfer at the D/A interface, and then recombination to ground state. The kinetic traces of PMZ-10:Y6 and PM6:Y6 were extracted and compared in **Figure 6d**, it is clear that hole transfer rate of PMZ-10:Y6 is higher than the PM6:Y6 blend, The faster CT process in the PMZ-10:Y6 blend may lead to higher yield of the CT state, which in turn generates higher photocurrent in the device. The results of fs-TA experiments are in good agreement with the better performance of the PMZ-10-based devices.

Conclusions

To conclude, we incorporate a low-cost electron-withdrawing PZ-T unit into PM6 polymer backbone as the third building component, and a series of high-performance D-A_1-D-A_2 type terpolymers were synthesized by random polymerization strategy. The three terpolymers are PMZ-10, PMZ-20 and PMZ-30 with the PZ-T proportion of 10%, 20% and 30%, respectively. With the increased proportion of PZ-T, the HOMO energy levels of the terpolymers down-shifted in comparison with PM6. In addition, the terpolymer-based active layers demonstrate efficient exciton dissociation, higher charge carrier mobility, and desirable aggregation behavior. Eventually, the optimized device based on PMZ-10:Y6 achieved the highest PCE of 18.23% (a certified PCE of 17.75% by NIM), which is the highest reported performance in the terpolymers-based PSCs. Therefore, the terpolymer strategy is proven to be a promising and efficient approach to develop high-performance polymer donors for the PSCs.

Acknowledgements

This work was supported by the National Key Research and Development Program of China (No. 2019YFA0705900) funded by MOST, NSFC (Nos. 51820105003, 21734008 and 61904181) and the Guangdong Major Project of Basic and Applied Basic Research (No. 2019B030302007). GIWAXS data were acquired at beam line 7.3.3 at the Advanced Light Source, which is supported by the Director, Office of Science, Office of Basic Energy

Sciences, of the U.S. Department of Energy under Contract No. DE-AC02-05CH11231.

Work by NCSU supported by ONR grant N000142012155.

Competing Interests

The authors declare no competing interests.

Reference

[1] Y. Li, Acc. Chem. Res. **2012**, 45, 723.

[2] C. Sun, S. Qin, R. Wang, S. Chen, F. Pan, B. Qiu, Z. Shang, L. Meng, C. Zhang, M. Xiao, C. Yang, Y. Li, J. Am. Chem. Soc. **2020**, 142, 1465.

[3] H. Yao, Y. Cui, D. Qian, C. S. Ponseca, Jr., A. Honarfar, Y. Xu, J. Xin, Z. Chen, L. Hong, B. Gao, R. Yu, Y. Zu, W. Ma, P. Chabera, T. Pullerits, A. Yartsev, F. Gao, J. Hou, J. Am. Chem. Soc. **2019**, 141, 7743.

[4] J. Hou, O. Inganas, R. H. Friend, F. Gao, Nat. Mater. **2018**, 17, 119.

[5] K. Jiang, Q. Wei, J. Y. L. Lai, Z. Peng, H. K. Kim, J. Yuan, L. Ye, H. Ade, Y. Zou, H. Yan, Joule **2019**, 3, 3020.

[6] D. Qian, Z. Zheng, H. Yao, W. Tress, T. R. Hopper, S. Chen, S. Li, J. Liu, S. Chen, J. Zhang, X. K. Liu, B. Gao, L. Ouyang, Y. Jin, G. Pozina, I. A. Buyanova, W. M. Chen, O.

Inganas, V. Coropceanu, J. L. Bredas, H. Yan, J. Hou, F. Zhang, A. A. Bakulin, F. Gao, Nat. Mater. **2018**, 17, 703.

[7] R. Kopecek, J. Libal, Nat. Energy **2018**, 3, 443.

[8] Q. Wei, W. Liu, M. Leclerc, J. Yuan, H. Chen, Y. Zou, Sci. China Chem. **2020**, 63, 1352.

[9] G. Zeng, J. Zhang, X. Chen, H. Gu, Y. Li, Y. Li, Sci. China Chem. **2019**, 62, 851.

[10] J. Yuan, C. Zhang, H. Chen, C. Zhu, S. H. Cheung, B. Qiu, F. Cai, Q. Wei, W. Liu, H. Yin, R. Zhang, J. Zhang, Y. Liu, H. Zhang, W. Liu, H. Peng, J. Yang, L. Meng, F. Gao, S. So, Y. Li, Y. Zou, Sci. China Chem. **2020**, 63, 1159.

[11] Y. Lin, J. Wang, Z. G. Zhang, H. Bai, Y. Li, D. Zhu, X. Zhan, Adv. Mater. **2015**, 27, 1170.

[12] J. Yuan, Y. Zhang, L. Zhou, G. Zhang, H.-L. Yip, T.-K. Lau, X. Lu, C. Zhu, H. Peng, P. A. Johnson, M. Leclerc, Y. Cao, J. Ulanski, Y. Li, Y. Zou, Joule **2019**, 3, 1140.

[13] C. Zhu, J. Yuan, F. Cai, L. Meng, H. Zhang, H. Chen, J. Li, B. Qiu, H. Peng, S. Chen, Energy Environ. Sci. **2020**, 13, 2459.

[14] G. Chai, Y. Chang, J. Zhang, X. Xu, L. Yu, X. Zou, X. Li, Y. Chen, S. Luo, B. Liu, F. Bai, Z. Luo, H. Yu, J. Liang, T. Liu, K. S. Wong, H. Zhou, Q. Peng, H. Yan, Energy Environ. Sci. **2021**, 14, 3469.

[15] W. Liu, X. Xu, J. Yuan, M. Leclerc, Y. Zou, Y. Li, ACS Energy Lett. **2021**, 6, 598.

[16] J. Yuan, T. Huang, P. Cheng, Y. Zou, H. Zhang, J. L. Yang, S. Y. Chang, Z. Zhang, W. Huang, R. Wang, D. Meng, F. Gao, Y. Yang, Nat. Commun. **2019**, 10, 570.

[17] L. Feng, J. Yuan, Z. Zhang, H. Peng, Z. G. Zhang, S. Xu, Y. Liu, Y. Li, Y. Zou, ACS Appl. Mater. Interfaces **2017**, 9, 31985.

[18] T. Ameri, J. Min, N. Li, F. Machui, D. Baran, M. Forster, K. J. Schottler, D. Dolfen, U. Scherf, C. J. Brabec, Adv. Energy Mater. **2012**, 2, 1198.

[19] Q. Fan, W. Su, Y. Wang, B. Guo, Y. Jiang, X. Guo, F. Liu, T. P. Russell, M. Zhang, Y. Li, Sci. China Chem. **2018**, 61, 531.

[20] C. Sun, F. Pan, H. Bin, J. Zhang, L. Xue, B. Qiu, Z. Wei, Z. G. Zhang, Y. Li, Nat. Commun. **2018**, 9, 743.

[21] C. Cui, Y. Li, Energy Environ. Sci. **2019**, 12, 3225.

[22] R. Ma, T. Liu, Z. Luo, Q. Guo, Y. Xiao, Y. Chen, X. Li, S. Luo, X. Lu, M. Zhang, Y. Li, H. Yan, Sci. China Chem. **2020**, 63, 325.

[23] G. Zhang, H. Ning, H. Chen, Q. Jiang, J. Jiang, P. Han, L. Dang, M. Xu, M. Shao, F. He, Q. Wu, Joule **2021**, 5, 1.

[24] C. Zhu, L. Meng, J. Zhang, S. Qin, W. Lai, B. Qiu, J. Yuan, Y. Wan, W. Huang, Y. Li, Adv. Mater. **2021**, 33, 2100474.

[25] Z. Shang, L. Zhou, C. Sun, L. Meng, W. Lai, J. Zhang, W. Huang, Y. Li, Sci. China Chem. **2021**, 64, 1031.

[26] C. Li, J. Zhou, J. Song, J. Xu, H. Zhang, X. Zhang, J. Guo, L. Zhu, D. Wei, G. Han, Nat. Energy **2021**, 6, 605.

[27] M. Zhang, L. Zhu, G. Zhou, T. Hao, C. Qiu, Z. Zhao, Q. Hu, B. W. Larson, H. Zhu, Z. Ma, Z. Tang, W. Feng, Y. Zhang, T. P. Russell, F. Liu, Nat. Commun. **2021**, 12, 309.

[28] T. Zhang, C. An, P. Bi, Q. Lv, J. Qin, L. Hong, Y. Cui, S. Zhang, J. Hou, Adv. Energy Mater. **2021**, 2101705.

[29] M. Zhang, X. Guo, W. Ma, H. Ade, J. Hou, Adv. Mater. **2015**, 27, 4655.

[30] X. Li, R. Ma, T. Liu, Y. Xiao, G. Chai, X. Lu, H. Yan, Y. Li, Sci. China Chem. **2020**, 9, 1256.

[31] L. Huo, X. Xue, T. Liu, W. Xiong, F. Qi, B. Fan, D. Xie, F. Liu, C. Yang, Y. Sun, Chem. Mater. **2018**, 30, 3294.

[32] I. Shin, H. j. Ahn, J. H. Yun, J. W. Jo, S. Park, S. y. Joe, J. Bang, H. J. Son, Adv. Energy Mater. **2018**, 8, 1701405.

[33] J.-W. Lee, M. J. Sung, D. Kim, S. Lee, H. You, F. S. Kim, Y.-H. Kim, B. J. Kim, S.-K. Kwon, Chem. Mater. **2020**, 32, 2572.

[34] D. Dang, D. Yu, E. Wang, Adv. Mater. **2019**, 31, 1807019.

[35] J. Lee, S. M. Lee, S. Chen, T. Kumari, S. H. Kang, Y. Cho, C. Yang, Adv. Mater. **2018**, 31, 1804762.

[36] H. Sun, T. Liu, J. Yu, T.-K. Lau, G. Zhang, Y. Zhang, M. Su, Y. Tang, R. Ma, B. Liu, J. Liang, K. Feng, X. Lu, X. Guo, F. Gao, H. Yan, Energy Environ. Sci. **2019**, 12, 3328.

[37] Y. Cui, H. Yao, L. Hong, T. Zhang, Y. Xu, K. Xian, B. Gao, J. Qin, J. Zhang, Z. Wei, J. Hou, Adv. Mater. **2019**, 31, 1808356.

[38] J. Wu, G. Li, J. Fang, X. Guo, L. Zhu, B. Guo, Y. Wang, G. Zhang, L. Arunagiri, F. Liu, H. Yan, M. Zhang, Y. Li, Nat. Commun. **2020**, 11, 4612.

[39] X. Guo, Q. Fan, J. Wu, G. Li, Z. Peng, W. Su, J. Lin, L. Hou, Y. Qin, H. Ade, Angew. Chem. Int. Ed. **2021**, 60, 2322.

[40] J.-W. Lee, D. Jeong, D. J. Kim, T. N.-L. Phan, J. S. Park, T.-S. Kim, B. J. Kim, Energy Environ. Sci. **2021**, 14, 4067.

[41] F. C. Spano, Acc. Chem. Res. **2010**, 43, 429.

[42] M. Más-Montoya, R. A. Janssen, Adv. Funct. Mater. **2017**, 27, 1605779.

[43] P. Schilinsky, C. Waldauf, C. J. Brabec, Appl. Phys. Lett. **2002**, 81, 3885.

[44] Y. Yang, Z. G. Zhang, H. Bin, S. Chen, L. Gao, L. Xue, C. Yang, Y. Li, J. Am. Chem. Soc. **2016**, 138, 15011.

[45] L. Lu, T. Xu, W. Chen, E. S. Landry, L. Yu, Nat. Photonics **2014**, 8, 716.

[46] A. Hexemer, W. Bras, J. Glossinger, E. Schaible, E. Gann, R. Kirian, A. MacDowell, M. Church, B. Rude, H. Padmore, J. Phys: Conf. Ser. **2010**, 247, 012007.

[47] X. Zou, G. Wen, R. Hu, G. Dong, C. Zhang, W. Zhang, H. Huang, W. Dang, Molecules **2020**, 25, 4118.

[48] Q. Guo, Y. Liu, M. Liu, H. Zhang, X. Qian, J. Yang, J. Wang, W. Xue, Q. Zhao, X. Xu, W. Ma, Z. Tang, Y. Li, Z. Bo, Adv. Mater. **2020**, 32, 2003164.

Table of Contents

An electron-withdrawing PZ-T unit was employed to incorporate into PM6 polymer backbone as the third component, and a series of high-performance D-A_1-D-A_2 type terpolymers were synthesized by random copolymerization strategy. Among them, the PMZ-10:Y6 based PSCs achieved outstanding PCE of 18.23%, which is the highest reported performance among the terpolymer-based PSCs so far.